

Comparative Control Strategies of an Underactuated Aircraft Wing Model

Hayder F. N. Al-Shuka* , Basim A. R. Al-Bakri 

Department of Aeronautical Engineering, College of Engineering, University of Baghdad, Baghdad 10011, Iraq

Corresponding Author Email: dr.hayder.f.n@coeng.uobaghdad.edu.iq



Copyright: ©2025 The authors. This article is published by IETA and is licensed under the CC BY 4.0 license (<http://creativecommons.org/licenses/by/4.0/>).

<https://doi.org/10.18280/jesa.580120>

ABSTRACT

Received: 15 November 2024

Revised: 24 December 2024

Accepted: 10 January 2025

Available online: 31 January 2025

Keywords:

partial feedback linearization, energy-based control, flatness-based control, servo constraints, underactuation, aeroelasticity

This paper describes four fundamental control schemes for a 2D aeroelastic wing model under quasi-steady flow conditions: partial feedback linearization control (PFLC), energy-based control (EC), flatness-based control (FC), and servo-constraint based feedforward control (SCFC). PFLC effectively categorizes degrees of freedom (DOFs) into active and passive groups, controlling the active DOFs while letting the stability of the passive joints depend on their internal dynamics. However, this approach has two limitations: the control law contains the inverse of the inertia matrix, and the evaluation of the internal stability of the passive joint dynamics is required. The control in EC is energy related - no more or less than the given energy - but the control law encounters problems with the computation of the energy inverse of the system. In contrast, FC linearizes the wing system and then obtains an output variable to be controlled; however, this method requires high-order derivatives of the system state, which can be very tedious. The strength of FC is that the controlled output can integrate most state variables. Kinematic constraints associated with the output to be produced are incorporated into the SCFC, and the equations of motion are reformulated to reflect the changes. Feedback and feedforward control terms come into play, as does the need to verify the stability of the internal dynamics of the control system. Modeling and simulation evaluations using MATLAB/SIMULINK confirmed that most of the control approaches were able to produce nearly similar dynamic responses with properly damped oscillations; however, the SCFC gives a fast response due to the presence of a feedforward term.

1. INTRODUCTION

Flexible aircraft structures offer improved efficiency, but their stability margins can be compromised. This instability results from the interaction of aerodynamic, inertial, and elastic forces. Nonlinearities in the wing structure, such as coupled bending, torsion, and elasticity, can lead to undesirable outcomes such as flutter and limit cycle oscillations [1-3]. Various models, including plates or shells with complex cross sections or an equivalent system with beams and flexible elements, are feasible [4]. This paper discusses the development of advanced nonlinear control strategies for aeroelastic systems. It describes the construction of a basic model that can be adapted using online feedback estimation techniques. The model aims to accurately capture the dynamic characteristics of the system while remaining simple. The aeroservoelastic (ASE) model is based on aerodynamic and structural principles for lifting surfaces, with an emphasis on simplifying assumptions of causality, linearity, and small perturbations. Complex aeroelastic models are not scalable for repeated online computations, so a linearized baseline model is sufficient. An ASE plant model utilizes a combination of steady, quasi-steady, or unsteady aerodynamics and small fluctuations in structural dynamics and can be represented in either integral or operational linear form. The basic plant structural model predicts aerodynamic

lift and pitch moments via simple Newtonian or Lagrange techniques. It is important to either find a closed-form solution of the unstable aerodynamics or perform an inversion of certain fundamental integral equations. However, accurate aerodynamic prediction may require the solution of nonlinear partial differential equations [4]. Therefore, this study focuses on modeling an aeroelastic wing based on an equivalent system with three degrees of freedom: pitch, aileron, and control surface coordinates. Using quasi-steady aerodynamics, the dynamics related to the control surface coordinate can be eliminated, and thus two DOF reduced wing models are developed.

A control system is important to attenuate wing vibrations. Vibration damping control can be classified into passive and active control strategies. Passive control schemes focus on modifications in wing geometry and aerodynamic characteristics, while active control requires actuators and sensors to regulate the wing oscillations. This research emphasizes the active control category. Miscellaneous control strategies have been used for attenuating the wing oscillations, such as adaptive decoupled fuzzy sliding control [5], control based on the tensor product model [6], output feedback control [7-9], the state-dependent Riccati equation method [10], linear quadratic Gaussian LQG [11], terminal sliding mode control [12, 13], synchronization theory [14], and adaptive neural control [15, 16]. In general, in most aeroservoelastic analyses

and applications of optimal control theory, the unsteady generalized forces are linearized, combined with controller dynamics and gust spectral models, and converted into linear state-space equations [17]. However, the linear control theory (e.g., PID control [18], pole placement [19], LGR/G [11, 20], and robust control [21]) might be insufficient to control the wing dynamics under nonlinear conditions such as free play, time delay, and bifurcation due to nonlinear structural stiffness [22]. Therefore, Kurdila et al. [23] provided a review of nonlinear control strategies for damping limit cycle oscillations of a nonlinear aeroelastic model. They focused on the use of partial feedback linearization control and MRAC, showing their characteristics and shortcomings. They concluded that the nonlinear MRAC seems to be more robust than the adaptive feedback linearization control under high flow velocities. However, other nonlinear control methods have been reported in the literature, such as gain scheduling scheme [24], inversion dynamic control [25], incremental inversion control [26], and recurrent neural control for system identification [27].

However, most of the above control techniques may not focus on the underactuation behavior of aircraft wings excepting the work of Ko and colleagues [23, 28, 29]. The number of control surfaces can affect the situation, leading to three potential actuation scenarios: an underactuated system, a fully actuated system, and an overactuated system [30]. This investigation delves into a challenging, underactuated case. Underactuated systems, which are mechanical systems with fewer control inputs than degrees of freedom, are found in a variety of applications, including flexible mobile and locomotive systems, robotics, aircrafts, and marines. The phenomenon of underactuation in systems can be because of actuator failure, engineering and robotic control design intentionally, and the internal dynamics of the system [31]. Therefore, this study develops and designs four control strategies for flexible wing structures to suppress aeroelastic instabilities: PFLC, EC, FC, and SCFC. Each method presents certain benefits concerning certain parts of the system's dynamic behavior; thus, they are examined in relation to their performance in oscillation control and system management of underactuation. The details on each control scheme are presented below. To our knowledge, literature reported using PFLC for regulation of oscillations of underactuated wings [28, 29], while the EC, FC, and the SCFC have been used in robotic systems extensively.

(1) The PFLC. An efficient approach eliminates the nonlinearities through the design of a suitable control law feedback loop. This method divides the degrees of freedom (DOFs) into active and passive. Active DOFs are controlled while passive joints may remain internally stable as regulated by the internal dynamics. This is very important where the number of inputs is less than that of the degrees of freedom. Having this controller for the design of the active DOFs control assures that the active DOFs are controlled with stability and accuracy. This technique has been used in regulating oscillations of most underactuated wing models [23, 28, 29] and also in several other robotic systems such as inverted pendulums, floating base and flexible base robots, and mobile robots [31-34]. The control of many systems at present is associated with the theory of feedback linearization, which is exact in most cases. Computed torque control in robotics is developed based on the concept of input-output linearization. Nonetheless, there are limitations when using such approaches in practice related to singularities or non-

linear mistake cancellation, and when the system is not in the minimal phase and has zero dynamics, which can lead to unstable control of the closed loops. The maximal linearization issue concerns the notion of flatness and the ability to construct an output with a relatively high degree.

(2) The EC. A universal stabilizing strategy adjusts the energy of underactuated manipulators using state feedback in order to reach closed-loop systems with desired stable states. It includes two major approaches: the controlled Lagrange method, which generates certain kinetic or potential energy from the Lie group, and the IDA-PBC method, which extends the controlled Lagrange methodology. The controlled Lagrange method is considered a complicated procedure where the simultaneous reconstruction of kinetic and potential energy is not undertaken. On the contrary, IDA-PBC is capable of reconstructing both energies with ease and has a relatively less sophisticated construction mechanism with its control law integrating energy reconstruction and input modulation. Over the recent years, the developments in the IDA-PBC methodology have offered better theoretical approaches as well as extended usability [35-38]. Despite this improvement, the two methods still consider a feedback control law that involves solving a series of partial differential equations to achieve it, which is problematic for handling systems with such simple nonlinear features and limits their use as well. In general, it encompasses the management of mechanical energy, the control of active variables, and the limitation of passive ones. For this, no more complicated mathematical formulation is needed than the one envisaging potential and kinetic energy for the concrete dynamical system at hand. Furthermore, this is not a case of partial feedback linearization since the latter only attempts to control the output in the presence of the active control surfaces. The simplicity of the controller being determined from the mechanical energy of the system is one of the benefits of energy-based methods. The controller is constructed from the energy storage function and guarantees the asymptotic stability of the system's equilibrium. Nevertheless, the non-actuated coordinate, which is not controlled directly by the system, will eventually tend to zero [39, 40].

(3) The FC. It is an improved method in system and control theory focusing on the control systems that are non-linear and where the control system of interest is not defined. It is based on the idea of "flat outputs" in the system; outputs depend on inputs, and all states and inputs are observable without integration. This is useful because the behavior of the system in question is determined by its outputs, which allows for precision in trajectory generation. When trajectory generation is required to be very accurate differential systems are used in order to connect the trajectories to the appropriate inputs [41]. In the study [42], a series of flat outputs are used to model the crane system dynamics with respect to certain constraints in fast positioning of the trolley and reduced swing angle. The ideal set of flat output parameters are obtained, and a tracking controller is designed to correct for any disturbances from wind. The backstepping controller, which is a control strategy based on flatness output, only adjusts some output of the system and thus can be applied to underactuated cranes since the output space and the flat output space can be connected through differentiable homeomorphisms. For more information on control to flattening, see the studies [43, 44].

(4) The SCFC. The blended use of feedforward and feedback control loops in the process of trajectory tracking in multibody systems offers a good practical solution to the

problem of performance versus stability. These permit the engineers to perform correct and fast trajectory tracking, even for complex systems with elastic elements. The feedforward control design aims at improving the tracking accuracy and response time of the system; in contrast, the feedback control design aims at stabilizing the system and making it robust to disturbances. That synergy is important in ensuring that trajectory tracking performance of multibody systems is enhanced at all times. In addition, simulated control is not always possible because an underactuated system can have more degrees of freedom than actuators, which will give rise to right half-plane zeros. This poses a research challenge as lightweight structures gain popularity for energy efficiency. The technique of inversion is widely used in the literature with various adaptations; see the studies [45-48] for more information. For the reason that underactuated systems have a smaller number of actuators, the overall dynamic model is presented in terms of partitioning coordinates into actuated and unactuated subsystems. The output path is therefore described as a superposition of actuated and unactuated coordinates with the aid of differential and algebraic phase for calculations. The algebraic part employs the dynamic sub-model with actuation coordinates, and suitable tuning parameters are used to maintain stability in internal dynamics. In the control design of multibody systems, it is common to use feedforward approaches to control partially controllable systems, which yields differential algebraic equations (DAEs). The servo-constraint method has been successfully applied to the dynamics of rigid bodies and is promising in differentially flat systems such as cranes and airplanes, as well as non-differentially flat systems such as passive joints and soft arms. Inverse modeling focuses on the system's internal dynamics, which can be examined with differential-geometric nonlinear control theory. Nowadays PFLC and EC approaches are not adequate for dealing with underactuated aeroelastic systems, due specifically to the presence of strong nonlinearities.

The present study is significant in that it makes contributions to the problem of underactuated aeroelastic wings by designing a simpler but still effective model and testing four advanced control strategies via simulations. The results are intended to guide the future evolution of aircraft structures that are lightweight and energy efficient but have to counteract aerodynamic instability. Lightweight, flexible airplanes exhibit aeroelastic behaviors that affect their performance when subjected to aerodynamic instabilities. Thus, this research proposes the implementation and assessment of advanced nonlinear control techniques in underactuated aeroelastic systems. The study focuses on four control schemes for a quasi-steady 2D aeroelastic wing model: (i) Partial Feedback Linearization Control (PFLC), (ii) Energy Control (EC), (iii) Flatness-based Control (FC), and (iv) Servo Constraints Feedforward Control (SCFC). PFLC utilizes the active degrees of freedom in control while employing passive dynamics to retain stability, although the method needs the inverse inertia matrix. EC Control incorporates the desired energy in the control in practice but has a problem of several computations. While FC removes the nonlinearity in the system under control, the control method has problems associated with external noise due to high-order derivatives of system states. SCFC introduced an output-dependent kinematic constraint, which subsequently changes the form of the motion equations and looks at the concept of stability. MATLAB/SIMULINK investigations showed that all techniques generate comparable overdamped responses;

however, SCFC could give a fast response due to the presence of a feedforward term.

The remainder of the paper is organized as follows: In Section 2, the dynamics of the quasi-steady 2D aeroelastic wing model is detailed. Control schemes are discussed in Section 3. Section 4 describes the simulation setups, results, and pertinent discussion. Finally, in Section 5, the conclusions and recommendations are specified.

2. DYNAMICS OF AN AEROELASTIC WING MODEL

This study investigates the mitigation of oscillations in the standard wing section shown in Figure 1. The airfoil is constrained by two degrees of freedom: pitch (θ) and plunge (δ). The system's equations of motion are formulated as follows [28-30].

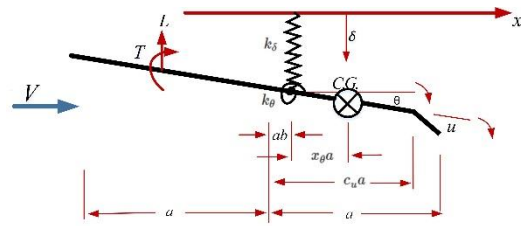


Figure 1. A two-DOF airfoil model

$$\begin{bmatrix} m & mx_{\theta}a \\ mx_{\theta}a & I_{\theta} \end{bmatrix} \begin{bmatrix} \ddot{\delta} \\ \ddot{\theta} \end{bmatrix} + \begin{bmatrix} c_{\delta} & 0 \\ 0 & c_{\theta} \end{bmatrix} \begin{bmatrix} \dot{\delta} \\ \dot{\theta} \end{bmatrix} + \begin{bmatrix} k_{\delta} & 0 \\ 0 & k_{\theta} \end{bmatrix} \begin{bmatrix} \delta \\ \theta \end{bmatrix} = \begin{bmatrix} -L \\ T \end{bmatrix} \quad (1)$$

where, the semichord, or reference length, is denoted by a , I_{θ} is the mass moment of inertia about the elastic axis, x_{θ} is the nondimensional distance between the center of mass and the elastic axis, m denotes the wing mass, and c_{δ} and c_{θ} are viscous damping coefficients related to plunge and pitch motions, respectively. The spring coefficients k_{δ} and k_{θ} correspond to the plunge and pitch motions, respectively. The aerodynamic force, L , and moment, T , have traditionally been modeled using a range of techniques, such as steady, quasi-steady, unsteady, and nonlinear aerodynamic models. This research investigates the aerodynamic force and moment in their quasi-steady form [28-30, 49, 50]. Aerodynamic models vary from simple steady-state-level analyses to unsteady models for the purpose of aeroelastic analysis. Modern CFD solvers are extremely demanding in computational power, which restricts their usage. Unsteady aerodynamic theory defines the lift and moment by separating its components into non-circulatory and circulatory parts. Non-circulatory components occur due to the acceleration of the fluid surrounding a body in motion and tend to negligibly small values when the density ratios are high enough. On the other hand, the circulatory components, which are dependent on the time history of the motion and types of wake, play an important role in the production of lift in the wings of airfoils. Many unsteady methodologies, however, lose their accuracy under certain conditions used, particularly during harmonic oscillations, which allows for convenient design of systems with low decay rates. Quasi-steady aerodynamic approximations are widely adopted in the pre-design stages of the project as the most straightforward modeling method. Their usage is deemed acceptable for flutter studies in certain directions of supersonic regimes. Quasi-

steady aerodynamics computes the forces influenced only by the present motion, forgetting all the previous motion and wakes. In general, this approach is widely used at the early stages in the analysis of aeroelasticity for predicting loads on lifting surfaces [51] or for calculating lift coefficients. Thus, the aerodynamic force and moments can be calculated as follows:

$$L = \sigma V^2 a c_{l_\theta} \left(\theta + \frac{\delta}{V} + \left(\frac{1}{2} - b \right) a \frac{\dot{\theta}}{V} \right) + \sigma V^2 a c_{l_u} u, \quad (2)$$

$$T = \sigma V^2 a c_{m_\theta} \left(\theta + \frac{\delta}{V} + \left(\frac{1}{2} - b \right) a \frac{\dot{\theta}}{V} \right) + \sigma V^2 a c_{m_u} u, \quad (3)$$

where, σ is the air density, V is the free stream velocity, b is a non-dimensional distance between the mid-chord and the elastic axis, c_{l_θ} and c_{l_u} are lift coefficients related to pitch coordinate and control surface angle, u , respectively, and c_{m_θ} and c_{m_u} are moment coefficients associated with pitch and control surface coordinates respectively. Aerodynamic coefficients are vital for measuring forces and moments on bodies in fluid flow. These non-dimensional quantities allow comparison of performance in aerodynamics with respect to many different objects and scenarios, which is more standard. It is common practice to normalize lifting, dragging, and other moment forces by dynamic pressure and reference parameters to obtain corresponding key coefficients. It is important to obtain all these coefficients when assessing and forecasting aerodynamic characteristics in different situations [52].

This study uses a quasi-steady aerodynamic model to analyze closed-loop system characteristics through feedback linearization. The simplified model's simplicity is emphasized, and the reduced frequency observed in experiments confirms the validity of the model. Substituting Eq. (2) and Eq. (3) into Eq. (1) yields:

$$\begin{aligned} & \begin{bmatrix} m & mx_\theta a \\ mx_\theta a & I_\theta \end{bmatrix} \begin{bmatrix} \delta \\ \dot{\theta} \end{bmatrix} \\ & + \begin{bmatrix} c_\delta + \sigma V a c_{l_\theta} & \sigma V a^2 c_{l_\theta} \left(\frac{1}{2} - b \right) \\ \sigma V a^2 c_{m_\theta} & c_\theta - \sigma V a^3 c_{m_\theta} \left(\frac{1}{2} - b \right) \end{bmatrix} \begin{bmatrix} \delta \\ \dot{\theta} \end{bmatrix} \\ & + \begin{bmatrix} k_\delta & \sigma V a^2 c_{l_\theta} \\ 0 & k_\theta - \sigma V a^2 c_{m_\theta} \end{bmatrix} \begin{bmatrix} \delta \\ \theta \end{bmatrix} = \begin{bmatrix} -\sigma a c_{l_u} V^2 u \\ \sigma a^2 c_{m_u} V^2 u \end{bmatrix} \end{aligned} \quad (4)$$

The highlighted (underlined) terms reveal the relationship between the aerodynamic forces and moments and the structural dynamics. The system presented in Eq. (4) is underactuated in the sense that it possesses two degrees of freedom while having only a single control input, making it a nonlinear control problem that requires choosing a suitable control law with caution. The existence of a control input signal in the two motion equations is inappropriate; thus, a coordinate or state transformation is required. By selecting the following state transformation based on partial feedback linearization [28-30]:

$$\varphi_1 = \delta, \varphi_2 = f_3 \theta - f_4 \delta \quad (5)$$

The state transformation in Eq. (5) will simplify the system significantly, transforming the coupled dynamics into a more tractable form. Eq. (4) becomes:

$$\begin{aligned} & \ddot{\varphi}_1 + \left[c_1 + c_2 \left(\frac{f_4}{f_3} \right) \right] \dot{\varphi}_1 + \left(\frac{c_2}{f_3} \right) \varphi_2 + k_1 \varphi_1 \\ & + \frac{1}{f_3} q_u(\varphi_1, \varphi_2)(\varphi_2 + f_4 \varphi_1) = f_3 V^2 u \end{aligned} \quad (6)$$

$$\begin{aligned} & \ddot{\varphi}_2 - \left[c_1 f_4 + c_2 \left(\frac{f_4^2}{f_3} \right) - c_3 f_3 - c_4 f_4 \right] \dot{\varphi}_1 \\ & - \left[c_2 \left(\frac{f_4}{f_3} \right) - c_4 \right] \dot{\varphi}_2 - (f_4 k_1 - f_3 k_3) \varphi_1 \end{aligned} \quad (7)$$

$$- \frac{1}{f_3} [f_4 q_u(\varphi_1, \varphi_2) - f_3 p_u(\varphi_1, \varphi_2)] (\varphi_2 + f_4 \varphi_1) = 0$$

Rewriting Eq. (6) in matrix form results in:

$$\begin{aligned} & \begin{bmatrix} 1 & 0 \\ 0 & 1 \end{bmatrix} \begin{bmatrix} \dot{\varphi}_1 \\ \dot{\varphi}_2 \end{bmatrix} + \begin{bmatrix} c_1 + c_2 \left(\frac{f_4}{f_3} \right) & (c_2/f_3) \\ -[c_1 f_4 + c_2 \left(\frac{f_4^2}{f_3} \right) - c_3 f_3 - c_4 f_4] & -[c_2 \left(\frac{f_4}{f_3} \right) - c_4] \end{bmatrix} \begin{bmatrix} \varphi_1 \\ \varphi_2 \end{bmatrix} \\ & + \begin{bmatrix} \frac{1}{f_3} q_u(\varphi_1, \varphi_2)(\varphi_2 + f_4 \varphi_1) \\ -(f_4 k_1 - f_3 k_3) \varphi_1 - \frac{1}{f_3} [f_4 q_u(\varphi_1, \varphi_2) - f_3 p_u(\varphi_1, \varphi_2)] (\varphi_2 + f_4 \varphi_1) \end{bmatrix} \begin{bmatrix} \varphi_1 \\ \varphi_2 \end{bmatrix} \\ & = \begin{bmatrix} f_3 V^2 u \\ 0 \end{bmatrix} \end{aligned} \quad (8)$$

where, system variables in Eq. (8) are defined as follows:

$$\begin{aligned} d &= m(I_\theta - mx_\theta^2 a^2) \\ k_1 &= I_\theta k_\delta / d \\ k_2 &= (I_\theta \sigma a c_{l_\theta} + mx_\theta a^3 \sigma c_{m_\theta}) / d \\ k_3 &= -mx_\theta a k_\delta / d \\ k_4 &= (-mx_\theta a^2 \sigma c_{l_\theta} - m \sigma a^2 c_{m_\theta}) / d \\ p(\theta) &= \left(-\frac{mx_\theta a}{d} \right) k_\theta(\theta) \\ q(\theta) &= \left(\frac{m}{d} \right) k_\theta(\theta) \\ c_1 &= [I_\theta (c_\delta + \sigma V a c_{l_\theta}) + mx_\theta \sigma V a^3 c_{m_\theta}] / d \\ c_2 &= [I_\theta \sigma V a^2 c_{l_\theta} \left(\frac{1}{2} - b \right) - mx_\theta a c_\theta + mx_\theta \sigma V a^4 c_{m_\theta} \left(\frac{1}{2} - b \right)] / d \\ c_3 &= (-mx_\theta a c_\delta - mx_\theta \sigma V a^2 c_{l_\theta} - m \sigma V a^2 c_{m_\theta}) / d \\ c_4 &= (m c_\theta - mx_\theta \sigma V a^3 c_{l_\theta} \left(\frac{1}{2} - b \right)) / d \\ f_3 &= (-I_\theta \sigma a c_{l_u} - mx_\theta a^3 \sigma c_{m_u}) / d \\ f_4 &= (mx_\theta a^2 \sigma c_{l_u} + m \sigma a^2 c_{m_u}) / d \end{aligned}$$

Let us assume we aim to regulate the plunge coordinate's movement (i.e., active) while maintaining the pitch coordinate's stability in the internal dynamics (i.e., passive). The connection between active and passive coordinates in dynamics can indirectly drive freely passive coordinates. The overall dynamic equation expressed in Eq. (8) can be rewritten as:

$$D(\varphi) \ddot{\varphi} + B(\varphi, \dot{\varphi}) + g(\varphi) = Au \quad (9)$$

with:

$$\begin{aligned} D(\varphi) &= \begin{bmatrix} 1 & 0 \\ 0 & 1 \end{bmatrix}, B(\varphi, \dot{\varphi}) \\ &= \begin{bmatrix} [c_1 + c_2 \left(\frac{f_4}{f_3} \right)] \dot{\varphi}_1 + (c_2/f_3) \dot{\varphi}_2 \\ -[c_1 f_4 + c_2 \left(\frac{f_4^2}{f_3} \right) - c_3 f_3 - c_4 f_4] \dot{\varphi}_1 - [c_2 \left(\frac{f_4}{f_3} \right) - c_4] \dot{\varphi}_2 \end{bmatrix} \end{aligned}$$

$$\begin{aligned} g(\varphi) = & \\ \left[\begin{array}{c} \frac{1}{f_3} q_u(\varphi_1, \varphi_2)(\varphi_2 + f_4 \varphi_1) \\ -(f_4 k_1 - f_3 k_3) \varphi_1 - \frac{1}{f_3} [f_4 q_u(\varphi_1, \varphi_2) - f_3 p_u(\varphi_1, \varphi_2)](\varphi_2 + f_4 \varphi_1) \end{array} \right] \\ , A = & \begin{bmatrix} f_3 V^2 & 0 \\ 0 & 0 \end{bmatrix}. \end{aligned}$$

3. CONTROL SCHEMES

3.1 Partial feedback linearization control

This method classifies the Degrees of Freedom (DOFs) as either active or passive and addresses control of active DOFs only, while the passive joints remain intact due to their internal dynamics. This is useful for underactuated systems that have more degrees of freedom than control inputs. Careful controller synthesis guarantees the capability of active DOF control with high stability and accuracy. Hence, once Eq. (9) is separated into active and passive coordinates, one can obtain the following relations:

$$\ddot{\varphi}_1 + B_a(\varphi, \dot{\varphi}) + g_a(\varphi) = f_3 V^2 u \quad (10)$$

$$\ddot{\varphi}_2 + B_p(\varphi, \dot{\varphi}) + g_p(\varphi) = 0 \quad (11)$$

where,

$$B_a(\varphi, \dot{\varphi}) = \left[c_1 + c_2 \left(\frac{f_4}{f_3} \right) \right] \dot{\varphi}_1 + \left(\frac{c_2}{f_3} \right) \dot{\varphi}_2,$$

$$g_a(\varphi) = \frac{1}{f_3} q_u(\varphi_1, \varphi_2)(\varphi_2 + f_4 \varphi_1),$$

$$\begin{aligned} B_p(\varphi, \dot{\varphi}) = & - \left[c_1 f_4 + c_2 \left(\frac{f_4^2}{f_3} \right) - c_3 f_3 - c_4 f_4 \right] \dot{\varphi}_1 \\ & - \left[c_2 \left(\frac{f_4}{f_3} \right) - c_4 \right] \dot{\varphi}_2, \end{aligned}$$

$$g_p(\varphi) = -(f_4 k_1 - f_3 k_3) \varphi_1 - \frac{1}{f_3} [f_4 q_u(\varphi_1, \varphi_2) - f_3 p_u(\varphi_1, \varphi_2)](\varphi_2 + f_4 \varphi_1).$$

Limitation on accelerations in Eq. (11) implies no applied torques at the passive joints. The principle of inverse dynamics control seeks to accomplish the opposite, which is to linearize the nonlinear system in Eq. (10) and Eq. (11) so that linear control techniques can be applied. For applying the known control input, it is easy to construct the control law from Eq. (10) when internal zero dynamics of the unactuated coordinate are considered in Eq. (11). The subsequent control law is thus chosen:

$$u = \frac{1}{f_3 V^2} (u_0 + B_a(\varphi, \dot{\varphi}) + g_a(\varphi)) \quad (12)$$

$$u_0 = \ddot{\varphi}_{d1} + K_d(\dot{\varphi}_{d1} - \dot{\varphi}_1) + K_p(\varphi_{d1} - \varphi_1) \quad (13)$$

where, the subscript d refers to desired references, K_d and K_p are positive feedback gains ensuring stability of the system. Substituting Eq. (12) and Eq. (13) into Eq. (10) yields the following closed loop dynamics.

$$(\ddot{\varphi}_{d1} - \ddot{\varphi}_1) + K_d(\dot{\varphi}_{d1} - \dot{\varphi}_1) + K_p(\varphi_{d1} - \varphi_1) = 0 \quad (14)$$

The system of Eq. (14) is stable as long as the gains K_p and K_d are positive. For details on stability of internal dynamics related to passive coordinates, see the studies [29, 53, 54].

3.2 Energy-based control

Partial feedback linearization enables us to meet our control objective to follow a predetermined reference trajectory for the controlled variables. However, is it feasible to improve this by controlling additional variables? The total body energy is another significant factor that is intimately associated with the movement of a system. In the studies [55, 56], the control of an underactuated mechanical system was considered with the main goal of controlling the total mechanical energy and some actuated variables of interest. The central question is whether it is possible to generate a control input that achieves the desired outcome.

$$\lim_{t \rightarrow 0} E_d - E = 0, \quad (15)$$

$$\lim_{t \rightarrow 0} \varphi_{1d} - \varphi_1 = 0, \lim_{t \rightarrow 0} \dot{\varphi}_1 = 0 \quad (16)$$

The task involves stabilizing actuated variables φ_1 and $\dot{\varphi}_1$ in Eq. (16) while controlling total mechanical energy E in Eq. (15), limiting unactuated variables φ_2 and $\dot{\varphi}_2$. To design a suitable controller based on the total mechanical energy of the system, we propose the following Lyapunov function candidate:

$$V = \frac{1}{2} (E - E_d)^2 + \frac{1}{2} K_d \dot{\varphi}_1^2 + \frac{1}{2} K_p \tilde{\varphi}_1^2 \quad (17)$$

Deriving the above along the trajectories of Eq. (9), we get:

$$\dot{V} = \dot{\varphi}_1 [(E - E_d)u + K_d \ddot{\varphi}_1 + K_p \tilde{\varphi}_1] \quad (18)$$

Let us select the control input, u , as:

$$(E - E_d)u + K_d \ddot{\varphi}_1 + K_p \tilde{\varphi}_1 = -\gamma \dot{\varphi}_1 \quad (19)$$

Then Eq. (18) becomes:

$$\dot{V} = -\gamma \dot{\varphi}_1^2 \leq 0. \quad (20)$$

From Eq. (10), we have:

$$\ddot{\varphi}_1 = f_3 V^2 u - B_a(\varphi, \dot{\varphi}) + g_a(\varphi) \quad (21)$$

Substituting Eq. (21) into Eq. (19) yields:

$$\begin{aligned} (E - E_d)u + K_d (f_3 V^2 u - B_a(\varphi, \dot{\varphi}) - g_a(\varphi)) \\ + K_p \tilde{\varphi}_1 = -\gamma \dot{\varphi}_1 \end{aligned} \quad (22)$$

According to Eq. (22), we can get the following control law:

$$u = \frac{1}{(E - E_d) + K_d f_3 V^2} (K_d B_a(\varphi, \dot{\varphi}) + K_d g_a(\varphi) - \gamma \dot{\varphi}_1 - K_p \tilde{\varphi}_1) \quad (23)$$

Remark 1. The total energy of the 2D wing model is calculated as:

$$E = \text{kinetic energy} + \text{potential energy} \\ = \frac{1}{2} \dot{q}^T M \dot{q} + \frac{1}{2} q^T K q \quad (24)$$

$$\text{where, } q = \begin{bmatrix} \delta \\ \theta \end{bmatrix}, M = \begin{bmatrix} m & mx_\theta a \\ mx_\theta a & I_\theta \end{bmatrix}, K = \begin{bmatrix} k_\delta & 0 \\ 0 & k_\theta \end{bmatrix}.$$

Therefore, the desired reference system energy can be computed in terms of the desired coordinates in Eq. (24).

3.3 Differential flatness-based control

It is a sophisticated strategy in control theory, especially advantageous for the nonlinear control systems of an unknown type. It is based on a notion of ‘‘flat outputs’’ in a system, where outputs correspond to the inputs, and all the states and inputs can be obtained without any integration. This is useful in generating trajectories accurately because the trajectory has output for the system. When trajectory generation accuracy is required, differential systems arise, allowing trajectory input correspondence instead [41]. Eq. (10) and Eq. (11) can be reformulated considering linear structural stiffness as follows:

$$\begin{aligned} \ddot{\varphi}_1 + a_{11}\dot{\varphi}_1 + a_{12}\dot{\varphi}_2 + a_{13}\varphi_1 + a_{14}\varphi_2 &= b_{11}u \\ \ddot{\varphi}_2 + a_{21}\dot{\varphi}_1 + a_{22}\dot{\varphi}_2 + a_{23}\varphi_1 + a_{24}\varphi_2 &= 0 \end{aligned} \quad (25)$$

Let $\varphi_1 = x_1, \dot{\varphi}_1 = x_2, \varphi_2 = x_3, \dot{\varphi}_2 = x_4$, then Eq. (25) can be expressed in a state space form as:

$$\dot{x} = Ax + Bu \quad (26)$$

$$\text{where, } A = \begin{bmatrix} 0 & 1 & 0 & 0 \\ -a_{13} & -a_{11} & -a_{14} & -a_{12} \\ 0 & 0 & 0 & 1 \\ -a_{23} & -a_{21} & -a_{24} & -a_{22} \end{bmatrix}, B = \begin{bmatrix} 0 \\ b_{11} \\ 0 \\ 0 \end{bmatrix}.$$

The flat output y of the linear system in (26) can be obtained as follows [41]:

$$y = [0 \ 0 \ \dots \ 1][B, AB \ \dots \ A^{n-1}B]^{-1}x \quad (27)$$

$$\begin{aligned} y &= (a_{21}x_4 + a_{21}^2x_1 - (a_{23} - a_{21}a_{22}))/d, \\ d &= b_{11}(a_{24}a_{21}^2 - a_{22}a_{21}a_{23} + a_{13}^2) \end{aligned} \quad (28)$$

The output y clearly parametrizes all system variables. To demonstrate this, we compute the time derivatives of y in succession until the control input u appears as follows:

$$\dot{y} = -\frac{a_{21}a_{23}}{d}x_1 - \frac{a_{21}a_{24}}{d}x_3 - \frac{a_{23}}{d}x_4 \quad (29)$$

$$\dot{y} = \frac{a_{23}^2}{d}x_1 + \frac{a_{23}a_{24}}{d}x_3 + \left(\frac{a_{23}a_{22} - a_{21}a_{24}}{d}\right)x_4 \quad (30)$$

$$\ddot{y} = d_1x_1 + d_2x_2 + d_3x_3 + d_4x_4 \quad (31)$$

$$\begin{aligned} y^{(4)} &= (-d_2a_{13} - d_4a_{23})x_1 \\ &+ (d_1 - d_2a_{21} - d_4a_{21})x_2 \\ &+ (-d_2a_{14} - d_4a_{24})x_3 + \\ &(d_2a_{12} + d_4a_{22})x_4 + d_2b_{11}u \end{aligned} \quad (32)$$

The control input can be determined from the last equation.

Remark 2. Due to the imposition of linear structural stiffness, Eq. (25) is linear in terms of state space form. Besides, the equations are regulated about set points of pitch and plunge coordinates that encourages using linearized model for the target system (in case some nonlinearity is included).

3.4 Servo constraints-based feedforward control

Servo constraints provide an effective way to model inversion through equations of constraints in output trajectory tracking. This is particularly beneficial in multibody system dynamics, where they extend traditional geometric constraints. A servo constraint can be incorporated into the equation of motion in Eq. (9) for tracking output variables. Consequently, the vibration of the aeroelastic wing model will be described as:

$$D(\varphi)\ddot{\varphi} + B(\varphi, \dot{\varphi}) + g(\varphi) = Au \quad (33a)$$

$$h(\varphi) - y_d = 0 \quad (33b)$$

There are two main methods to solve Eq. (33): projection and coordinate transformation methods (see the studies [46-48] for details). This section will focus on coordinate transformation for feedforward control design. Consider the following coordinate transformation:

$$\bar{\varphi} = \begin{bmatrix} y = h(\varphi) \\ \varphi_2 \end{bmatrix} = \alpha(\varphi) \quad (34)$$

Differentiation Eq. (34) twice leads to:

$$\dot{\bar{\varphi}} = H\dot{\varphi} \quad (35a)$$

$$\ddot{\bar{\varphi}} = H\ddot{\varphi} + \dot{H}\dot{\varphi} \quad (35b)$$

Substituting Eq. (33a) into Eq. (35b) leads to:

$$\begin{aligned} \ddot{\bar{\varphi}} &= \begin{bmatrix} \ddot{y} \\ \ddot{\varphi}_2 \end{bmatrix} \\ &= \begin{bmatrix} (HD^{-1}B)u - HD^{-1}((\varphi, \dot{\varphi}) + g(\varphi)) + \dot{H}\dot{\varphi} \\ [0 \ 1]D^{-1}(Bu - ((\varphi, \dot{\varphi}) + g(\varphi))) \end{bmatrix} \end{aligned} \quad (36)$$

The above equation represents the equation of motion for an underactuated aeroelastic airfoil denoted by the output variable y and the underactuated coordinate φ_2 . The control law can be designed from the first row of Eq. (36) for a given desired output as follows:

$$u = (HD^{-1}B)^{-1}(HD^{-1}((\varphi, \dot{\varphi}) + g(\varphi)) - \dot{H}\dot{\varphi} + \ddot{y}_d) \quad (37)$$

whereas the internal dynamics can be determined from the second row of Eq. (36) with inserting Eq. (37) into it to get:

$$\begin{aligned} \ddot{\varphi}_2 &= [0 \ 1]D^{-1} \left(B(HD^{-1}B)^{-1}(HD^{-1}((\varphi, \dot{\varphi}) \right. \\ &\quad \left. + g(\varphi)) - \dot{H}\dot{\varphi} + \ddot{y}_d) \right. \\ &\quad \left. - ((\varphi, \dot{\varphi}) + g(\varphi)) \right) \end{aligned} \quad (38)$$

Remark 3. (i) Other possible control techniques include coupling control [57] and backstepping control [58] to stabilize underactuated dynamic systems. (ii) It should be noted that the aforementioned control techniques presume the knowledge of system dynamics. Therefore, work on these techniques in adaptive versions is important for practice. As far as adaptive control and the schemes for its extensions are concerned, refer to [58-62].

4. SIMULATION RESULTS AND DISCUSSIONS

This section carefully provides a number of simulation studies designed to evaluate and compare four different control strategies applied to an underactuated two-dimensional 2D-wing model as presented in Figure 1. The parameters that define the geometry of the wing have been clearly outlined in Table 1, along with all the control parameters for the respective control techniques in Table 2 for ease of understanding. The gains can be selected gradually from small values to large ones, that makes instability in response, and then values are halved. In addition, the proposed control schemes do not consider the uncertainties related to system parameters and hence a system identification technique should be implemented in practice to estimate and verify the system modeling.

In order to activate the dynamics of the wing in simulation, it is also possible to create oscillations by introducing an impulse load or presetting a number of generalized coordinates of the wing to certain values. In this work, the duration of action of the impulse response of 10 N is chosen to be 0.1 s in order to create oscillations in the motion of a wing, whereby it is important that the conditions be set at the beginning of the process, which is from the rest position. The control techniques presented in this research are considered to be classical since they do not adapt and hence rely on considerable information regarding the physical parameters. Conversely, it would not be possible to carry out real-time experimentation without employing a system identification approach and adaptive control schemes to get the best possible output and performance.

Overall, five trials were carried out carefully, the results of which are depicted graphically in Figures 2-4 with respect to the responses concerning pitch, plunge, and control input, respectively. Experiment 1, first, focuses on the wing vibration mode of forced initial conditions with an open-loop system. This causes some important effects, for example, high-order oscillations and long settling times, which are very important for the evaluation of the system's dynamic performance. In Experiment 2, however, the emphasis shifts, and partial feedback linearization is applied with the goal of controlling the punch coordinate. At the same time, Eq. (11) is used to control certain internal dynamics related to the pitch angle of the wing. However, it is important to point out that while the use of partial feedback linearization usually entails the need for the inverse of the mass matrix, looking at the present results. We do not deal with that aspect, as Eq. (11) and Eq. (12) represent a significant reduction in complexity since they presume a mass coefficient equal to one, making the analysis straightforward. Next, Experiment 3 combines energy-based control in Eq. (23) for the common purpose of mitigating oscillations by employing energy in the control scheme. However, it was noted that substantial issues may be encountered in the computations when the energy value nears

zero, hence resulting in very high control inputs, which can make the system unstable. In experiment four, a flatness-based approach is employed in which control is linearized with respect to certain equilibrium points, and the control implemented is from Eqs. (28)-(32). This approach has a formulation that uses state variables of order four and states that this way of working in the real world may be problematic as it leads to very high-frequency signals, which make it hard to control the system. Finally, experiment number five describes a simulation of the wing using the closed-loop control method with servo limitations. In this instance, the controller given by Eq. (37) is built by combining feedback with feedforward in an effort to improve the overall performance of the control system. On the other hand, the weakness of this approach is that the inverse matrix, which has to be computed in this approach, can lead to problems of computational singularity affecting the smoothness and reliability of control. The big feature of this technique is the fast response of the response compared with the rest of them.

Table 1. Physical parameters used in simulation experiments [7]

Parameter	Value
A	0.135 m
m	12.4
I_θ	0.07 kg.m ²
r_{cg}	0.09-(a+b.a)
x_θ	r_{cg}/a
ρ	1.23 kg/m ³
$span$	0.6 m
c_{l_θ}	6.3
k_δ	2844 N/m
c_{l_u}	3.36
c_δ	27.4 Ns/m
c_{m_θ}	$(0.5+b) c_{l_\alpha}$
c_{m_u}	-0.6
k_θ	2.82

Table 2. Control gains used in the selected control methods

Control Method	Gain Values
PFLC	$K_p=200, K_d=50$
EC	$K_p=300, K_d=75$
FC	The characteristic polynomial selected is $s^2 + 2\xi w_n s + w_n^2$ with $\xi=0.7$ and $w_n=0.8$
SCFC	Here only a feedforward control term is used.

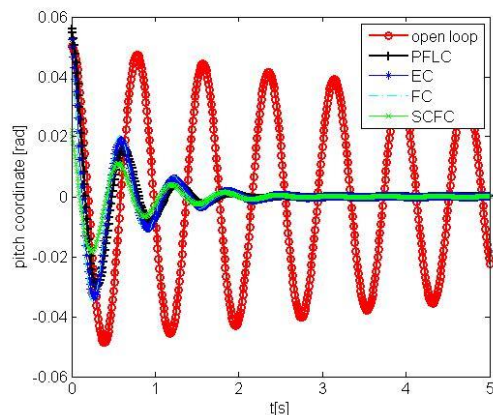


Figure 2. Pitch response

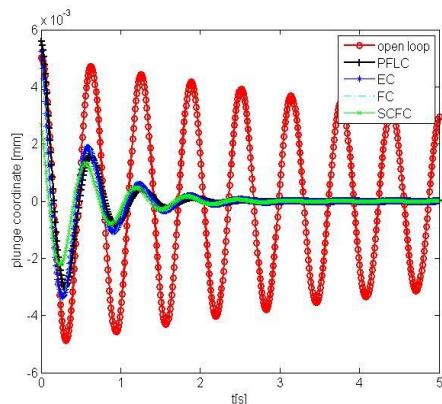


Figure 3. Plunge response

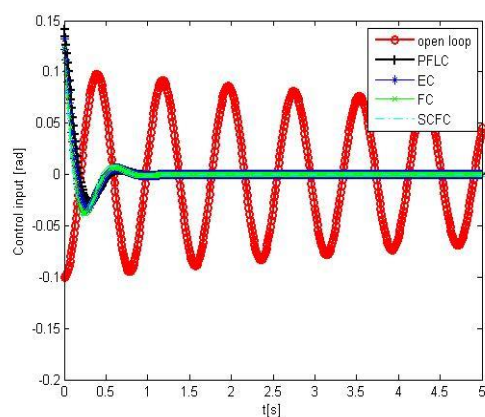


Figure 4. Control input response

5. CONCLUSIONS

This paper investigates the effectiveness of the following control techniques in smoothing the responses of a two-dimensional configuration of an aeroelastic wing in quasi-

steady flow: PFLC, EC, FC, and SCFC. PFLC manages the controlled degrees of freedom by utilizing the system's innate stability due to the presence of passively controlled joints. However, it is also available for active joint control only, requiring a full passive stability analysis and the property of an inertia matrix's inverse. EC control law embeds a desired energy value in the physical formulation and aims to control energy states. However, it might be quite difficult or even impossible to realize such an approach in applications. After formulating output terminal specifications, linearizing flatness control is used without concern about how well the actual system will follow the dynamics enclosing these outputs, but it ignores the fact that high-order state derivatives are subject to noise and, even if available, significantly degrade control performance. On the other hand, SCFC transforms motion equations in order to impose kinematic constraints and fuses feedback and feedforward methods in the control of kinematic motions, which requires a thorough assessment of the stability of internal dynamics. The different control methods mentioned above have their own advantages, but they also bring limitations which should be scrutinized thoroughly. A detailed analysis of adaptive control varieties may then be necessary in order to check with the real practicality of each of these approaches. All the investigated control methods in this paper are sensitive to disturbance and system uncertainty; however, the SCFC could give better performance and faster response due to the presence of a feedforward term. See Table 3 for a comparison between the above-mentioned control schemes.

Attention could also be given to several aspects in order to improve these control schemes in one way or another. One such expansion seems to be the addition of actuator mechanical dynamics to the dynamic model of the wing, making such a system three active controlled degrees of freedom with one actuation schema. In addition, taking into account the architectural control system disturbances, such as gust and jet effects, is important since these influences may significantly degrade the performance of the system. Lastly, the combination of smart control methods and the continuous model of the wing might prove beneficial in increasing the adaptability and reactivity of the system in operation.

Table 3. Comparison of the above-mentioned control methods

Feedback Linearization	Energy-Based Control	Flatness-Based Control	Servo Constraints-Based Feedforward Control
1. The goal is to design a nonlinear control law that can cancel the nonlinearity in the closed-loop dynamics.	1. The goal is to inject the system energy dynamics in the control law.	1. The goal is to select flat outputs to generate control law.	1. The goal is to use servo constraints to achieve precise control with a fast response.
2. It is a model-based approach.	2. It is a model-based scheme that requires calculation of system energy dynamics in Lyapunov function.	2. It is a model-based scheme.	2. It is a model-based approach.
3. It needs full or partial state variables in control law structure.	3. It could not require a full state feedback.	3. It could not require a full state feedback.	3. Use a feedforward state term for precise tracking.
4. The challenges lie in points (2) and (3) mentioned above.	4. The challenge lies in point (2) mentioned above for complex systems.	4. Capturing the flat outputs could be difficult for complex systems.	4. Sensitive to changing conditions and disturbances.

REFERENCES

[1] Nguyen, N., Tuzcu, I., Yucelen, T., Calise, A. (2011). Longitudinal dynamics and adaptive control application for an aeroelastic generic transport model. In AIAA

Atmospheric Flight Mechanics Conference, p. 6291. <https://doi.org/10.2514/6.2011-6291>
 [2] Ansari, A.R., Novinzadeh, A.R.B. (2017). Designing a control system for an airplane wing flutter employing gas actuators. International Journal of Aerospace

- Engineering, 2017(1): 4209619. <https://doi.org/10.1155/2017/4209619>
- [3] Ding, Q., Wang, D.L. (2006). The flutter of an airfoil with cubic structural and aerodynamic non-linearities. *Aerospace Science and Technology*, 10(5): 427-434. <https://doi.org/10.1016/j.ast.2006.03.005>
- [4] Tewari, A. (2016). *Adaptive Aeroservoelastic Control*. John Wiley & Sons.
- [5] Lin, C.M., Chin, W.L. (2006). Adaptive decoupled fuzzy sliding-mode control of a nonlinear aeroelastic system. *Journal of Guidance, Control, and Dynamics*, 29(1): 206-209. <https://doi.org/10.2514/1.17152>
- [6] Baranyi, P. (2006). Tensor product model-based control of two-dimensional aeroelastic system. *Journal of Guidance, Control, and Dynamics*, 29(2): 391-400. <https://doi.org/10.2514/1.9462>
- [7] Baranyi, P. (2006). Output feedback control of two-dimensional aeroelastic system. *Journal of Guidance, Control, and Dynamics*, 29(3): 762-767. <https://doi.org/10.2514/1.14981>
- [8] Singh, S.N., Wang, L. (2002). Output feedback form and adaptive stabilization of a nonlinear aeroelastic system. *Journal of Guidance, Control, and Dynamics*, 25(4): 725-732. <https://doi.org/10.2514/2.4939>
- [9] Xing, W., Singh, S.N. (2000). Adaptive output feedback control of a nonlinear aeroelastic structure. *Journal of Guidance, Control, and Dynamics*, 23(6): 1109-1116. <https://doi.org/10.2514/2.4662>
- [10] Bhoir, N., Singh, S.N. (2005). Control of unsteady aeroelastic system via state-dependent Riccati equation method. *Journal of Guidance, Control, and Dynamics*, 28(1): 78-84. <https://doi.org/10.2514/1.6590>
- [11] Ouyang, Y., Gu, Y., Kou, X., Yang, Z. (2021). Active flutter suppression of wing with morphing flap. *Aerospace Science and Technology*, 110: 106457. <https://doi.org/10.1016/j.ast.2020.106457>
- [12] Chen, C.L., Chang, C.W., Yau, H.T. (2012). Terminal sliding mode control for aeroelastic systems. *Nonlinear Dynamics*, 70: 2015-2026. <https://doi.org/10.1007/s11071-012-0593-x>
- [13] Liu, S., Yang, C., Zhang, Q., Whidborne, J.F. (2024). Disturbance observer-based backstepping terminal sliding mode aeroelastic control of airfoils. *Aerospace*, 11(11): 882. <https://doi.org/10.3390/aerospace11110882>
- [14] Vishal, S., Raaj, A., Bose, C., Venkatramani, J. (2021). Routes to synchronization in a pitch-plunge aeroelastic system with coupled structural and aerodynamic nonlinearities. *International Journal of Non-Linear Mechanics*, 135: 103766. <https://doi.org/10.1016/j.ijnonlinmec.2021.103766>
- [15] Tang, D., Chen, L., Tian, Z.F., Hu, E. (2021). A neural network approach for improving airfoil active flutter suppression under control-input constraints. *Journal of Vibration and Control*, 27(3-4): 451-467. <https://doi.org/10.1177/1077546320929153>
- [16] Prabhu, L., Srinivas, J. (2015). Robust control of a three degrees of freedom aeroelastic model using an intelligent observer. In *2015 International Conference on Robotics, Automation, Control and Embedded Systems (RACE)*, pp. 1-5. <https://doi.org/10.1109/RACE.2015.7097251>
- [17] Mukhopadhyay, V. (2003). Historical perspective on analysis and control of aeroelastic responses. *Journal of Guidance, Control, and Dynamics*, 26(5): 673-684. <https://doi.org/10.2514/2.5108>
- [18] Na, S., Song, J.S., Choo, J.H., Qin, Z. (2011). Dynamic aeroelastic response and active control of composite thin-walled beam structures in compressible flow. *Journal of Sound and Vibration*, 330(21): 4998-5013. <https://doi.org/10.1016/j.jsv.2011.05.026>
- [19] Ricci, S., Scotti, A., Cecrdle, J., Malecek, J. (2008). Active control of three-surface aeroelastic model. *Journal of Aircraft*, 45(3): 1002-1013. <https://doi.org/10.2514/1.33303>
- [20] Karpel, M. (1982). Design for active flutter suppression and gust alleviation using state-space aeroelastic modeling. *Journal of Aircraft*, 19(3): 221-227. <https://doi.org/10.2514/3.57379>
- [21] Poussot-Vassal, C., Demourant, F., Lepage, A., Le Bihan, D. (2016). Gust load alleviation: Identification, control, and wind tunnel testing of a 2-D aeroelastic airfoil. *IEEE Transactions on Control Systems Technology*, 25(5): 1736-1749. <https://doi.org/10.1109/TCST.2016.2630505>
- [22] Schildkamp, R., Chang, J., Sodja, J., De Breuker, R., Wang, X. (2023). Incremental nonlinear control for aeroelastic wing load alleviation and flutter suppression. *Actuators*, 12(7): 280. <https://doi.org/10.3390/act12070280>
- [23] Kurdila, A.J., Strganac, T.W., Junkins, J.L., Ko, J., Akella, M.R. (2001). Nonlinear control methods for high-energy limit-cycle oscillations. *Journal of Guidance, Control, and Dynamics*, 24(1): 185-192. <https://doi.org/10.2514/2.4700>
- [24] Lhachemi, H., Chu, Y., Saussié, D., Zhu, G. (2017). Flutter suppression for underactuated aeroelastic wing section: Nonlinear gain-scheduling approach. *Journal of Guidance, Control, and Dynamics*, 40(8): 2102-2109. <https://doi.org/10.2514/1.G002497>
- [25] Platanitis, G., Strganac, T.W. (2004). Control of a nonlinear wing section using leading-and trailing-edge surfaces. *Journal of Guidance, Control, and Dynamics*, 27(1): 52-58. <https://doi.org/10.2514/1.9284>
- [26] Wang, X., Van Kampen, E.J., Chu, Q., Lu, P. (2019). Stability analysis for incremental nonlinear dynamic inversion control. *Journal of Guidance, Control, and Dynamics*, 42(5): 1116-1129. <https://doi.org/10.2514/1.G003791>
- [27] Mataboni, M., Quaranta, G., Mantegazza, P. (2009). Active flutter suppression for a three-surface transport aircraft by recurrent neural networks. *Journal of Guidance, Control, and Dynamics*, 32(4): 1295-1307. <https://doi.org/10.2514/1.40774>
- [28] Ko, J., Kurdila, A.J., Strganac, T.W. (1997). Nonlinear control of a prototypical wing section with torsional nonlinearity. *Journal of Guidance, Control, and Dynamics*, 20(6): 1181-1189. <https://doi.org/10.2514/2.4174>
- [29] Ko, J., Strganac, T.W., Kurdila, A.J. (1998). Stability and control of a structurally nonlinear aeroelastic system. *Journal of Guidance, Control, and Dynamics*, 21(5): 718-725. <https://doi.org/10.2514/2.4317>
- [30] Al-Shuka, H.F., Corves, B. (2023). Function approximation technique (FAT)-based adaptive feedback linearization control for nonlinear aeroelastic wing models considering different actuation scenarios. *Mathematical Models and Computer Simulations*, 15(1): 152-166. <https://doi.org/10.1134/S2070048223010106>

- [31] Xin, X., Liu, Y. (2014). Control design and analysis for underactuated robotic systems. Okayama: Springer London.
- [32] Pathak, K., Franch, J., Agrawal, S.K. (2005). Velocity and position control of a wheeled inverted pendulum by partial feedback linearization. *IEEE Transactions on Robotics*, 21(3): 505-513. <https://doi.org/10.1109/TRO.2004.840905>
- [33] Maalouf, D., Moog, C. H., Aoustin, Y., Li, S. (2015). Classification of two-degree-of-freedom underactuated mechanical systems. *IET Control Theory & Applications*, 9(10): 1501-1510. <https://doi.org/10.1049/iet-cta.2014.0280>
- [34] Liu, Y., Yu, H. (2013). A survey of underactuated mechanical systems. *IET Control Theory & Applications*, 7(7): 921-935. <https://doi.org/10.1049/iet-cta.2012.0505>
- [35] Bloch, A.M., Leonard, N.E., Marsden, J.E. (2000). Controlled Lagrangians and the stabilization of mechanical systems. I. The first matching theorem. *IEEE Transactions on Automatic Control*, 45(12): 2253-2270. <https://doi.org/10.1109/9.895562>
- [36] Bloch, A.M., Chang, D.E., Leonard, N.E., Marsden, J.E. (2001). Controlled Lagrangians and the stabilization of mechanical systems. II. Potential shaping. *IEEE Transactions on Automatic Control*, 46(10): 1556-1571. <https://doi.org/10.1109/9.956051>
- [37] Ortega, R., Spong, M.W. (2000). Stabilization of underactuated mechanical systems via interconnection and damping assignment. *IFAC Proceedings Volumes*, 33(2): 69-74. [https://doi.org/10.1016/S1474-6670\(17\)35549-0](https://doi.org/10.1016/S1474-6670(17)35549-0)
- [38] Gomez-Estern, F., Ortega, R., Rubio, F.R., Aracil, J. (2001). Stabilization of a class of underactuated mechanical systems via total energy shaping. In *Proceedings of the 40th IEEE Conference on Decision and Control (Cat. No. 01CH37228)*, 2: 1137-1143. <https://doi.org/10.1109/CDC.2001.981038>
- [39] Dong, Y., Wang, Z., Feng, Z., Wang, D., Fang, H. (2008). Energy-based control for a class of under-actuated mechanical systems. In *2008 Congress on Image and Signal Processing*, 3: 139-143. <https://doi.org/10.1109/CISP.2008.304>
- [40] Hoang, N.Q., Lee, S.G., Kim, J.J., Kim, B.S. (2014). Simple energy-based controller for a class of underactuated mechanical systems. *International Journal of Precision Engineering and Manufacturing*, 15: 1529-1536. <https://doi.org/10.1007/s12541-014-0501-z>
- [41] Sira-Ramirez, H., Agrawal, S.K. (2018). *Differentially Flat Systems*. CRC Press.
- [42] Yu, Z., Niu, W. (2023). Flatness-based backstepping antisway control of underactuated crane systems under wind disturbance. *Electronics*, 12(1): 244. <https://doi.org/10.3390/electronics12010244>
- [43] Rigatos, G., Pomares, J., Siano, P., AL-Numay, M., Abbaszadeh, M., Cuccurullo, G. (2024). Flatness-based control in successive loops for mechatronic motion transmission systems. *Asian Journal of Control*, 26(6): 2807-2842, <https://doi.org/10.1002/asjc.3378>
- [44] Ma, S.F., Zhao, A., Sun, J.Q. (2024). Identification of linear flat outputs using neural networks—Examples of two-degree-of-freedom underactuated mechanical systems. *Mechanical Systems and Signal Processing*, 216: 111471. <https://doi.org/10.1016/j.ymssp.2024.111471>
- [45] Devasia, S., Chen, D., Paden, B. (1996). Nonlinear inversion-based output tracking. *IEEE Transactions on Automatic Control*, 41(7): 930-942. <https://doi.org/10.1109/9.508898>
- [46] Seifried, R. (2012). Two approaches for feedforward control and optimal design of underactuated multibody systems. *Multibody System Dynamics*, 27: 75-93. <https://doi.org/10.1007/s11044-011-9261-z>
- [47] Seifried, R. (2010). Optimization-based design of minimum phase underactuated multibody systems. In *Multibody Dynamics: Computational Methods and Applications*, pp. 261-282. https://doi.org/10.1007/978-90-481-9971-6_13
- [48] Seifried, R. (2012). Integrated mechanical and control design of underactuated multibody systems. *Nonlinear Dynamics*, 67: 1539-1557. <https://doi.org/10.1007/s11071-011-0087-2>
- [49] Dimitriadis, G. (2017). *Introduction to Nonlinear Aeroelasticity*. John Wiley & Sons.
- [50] Wright, J.R., Cooper, J.E. (2008). *Introduction to Aircraft Aeroelasticity and Loads*. John Wiley & Sons.
- [51] Haddadpour, H., Firouz-Abadi, R.D. (2006). Evaluation of quasi-steady aerodynamic modeling for flutter prediction of aircraft wings in incompressible flow. *Thin-Walled Structures*, 44(9): 931-936. <https://doi.org/10.1016/j.tws.2006.08.020>
- [52] Grande, A., Martínez, S., Piqué, I., Tononi, J., Tugores, F. (2017). Aerodynamic's measurements of wing's parameters. Aerospace Engineering Division, Physics Department, Campus del Baix Llobregat, Castelldefels, Catalunya. <http://hdl.handle.net/2117/192010>.
- [53] Lanza, L. (2021). Representation and stability of internal dynamics. *Proceedings. Applied Mathematics Mechanics*, 20(1): e202000256. <https://doi.org/10.1002/pamm.202000256>
- [54] Yun, X., Yamamoto, Y. (1997). Stability analysis of the internal dynamics of a wheeled mobile robot. *Journal of Robotic Systems*, 14(10): 697-709. [https://doi.org/10.1002/\(SICI\)1097-4563\(199710\)14:10<697::AID-ROB1>3.0.CO;2-P](https://doi.org/10.1002/(SICI)1097-4563(199710)14:10<697::AID-ROB1>3.0.CO;2-P)
- [55] Fantoni, I., Lozano, R. (2012). *Non-Linear Control for Underactuated Mechanical Systems*. Springer Science & Business Media.
- [56] Kolesnichenko, O., Shiriaev, A.S. (2002). Partial stabilization of underactuated Euler–Lagrange systems via a class of feedback transformations. *Systems & Control Letters*, 45(2): 121-132. [https://doi.org/10.1016/S0167-6911\(01\)00170-0](https://doi.org/10.1016/S0167-6911(01)00170-0)
- [57] Reyhanoglu, M., Hoffman, D. (2016). Modeling and control of a flexible-structure-mounted manipulator. In *2016 IEEE International Conference on Advanced Intelligent Mechatronics (AIM)*, Banff, AB, Canada, pp. 953-957. <https://doi.org/10.1109/AIM.2016.7576892>
- [58] Fu, M. (2023). Control of the cart-pole system: Model-based vs. model-free learning. *IFAC-PapersOnLine*, 56(2): 11847-11852. <https://doi.org/10.1016/j.ifacol.2023.10.588>
- [59] Al-Shuka, H.F., Corves, B. (2023). Function approximation technique (FAT)-based adaptive feedback linearization control for nonlinear aeroelastic wing models considering different actuation scenarios. *Mathematical Models and Computer Simulations*, 15(1): 152-166. <https://doi.org/10.1134/S2070048223010106>

[60] Al-Shuka, H.F., Corves, B., Abbas, E.N. (2023). Cascade position-torque control strategy based on function approximation technique (FAT) for flexible joint robots. AIP Conference Proceedings, 2651(1): 050007. <https://doi.org/10.1063/5.0105424>

[61] Al-Shuka, H.F., Kaleel, A.H., Al-Bakri, B.A. (2024). Hierarchical stabilization and tracking control of a flexible-joint bipedal robot based on anti-windup and adaptive approximation control. Journal of Robotics, 2024(1): 6692666. <https://doi.org/10.1155/2024/6692666>

[62] Al-Shuka, H.F., Abbas, E. (2022). Function approximation technique (FAT)-based nonlinear control strategies for smart thin plates with cubic nonlinearities. FME Transactions, 50(1): 168-180. <https://doi.org/10.5937/fme2201168.hal-03721791>

NOMENCLATURE

- a the semichord, or reference length, m
- b a non-dimensional distance between the mid-chord and the elastic axis
- c_δ viscous damping coefficient related to plunge coordinate, ns/m
- c_θ viscous damping coefficient related to plunge coordinate, n rad s/rad

- c_{l_θ} a dimensionless lift coefficient related to pitch coordinate
- c_{l_u} a dimensionless lift coefficient related to control surface angle
- c_{m_θ} a dimensionless moment coefficient associated with pitch
- c_{m_u} a dimensionless moment coefficient associated with control surface coordinate
- I_θ the mass moment of inertia of the wing about the elastic axis, kg.m²
- k_δ spring (structural) stiffness coefficient related to plunge coordinate, n/m
- k_θ spring (structural) stiffness coefficient related to pitch coordinate, nm/rad
- L aerodynamic force, n
- m the mass of the wing, kg
- T aerodynamic torque, nm
- u control surface angle related to flap
- V free stream velocity
- x_θ the nondimensional distance between the center of mass and the elastic axis

Greek symbols

- δ plunge coordinate, m
- θ pitch coordinate, rad
- σ air density, kg.m⁻³